DOI: 10.1002/ejic.200900017

Systematic Electronic Control in Ambipolar Compounds Optimizes Their Photoluminescence Properties: Synthesis, Characterization, and Device Fabrication of Four-Coordinate Boron Compounds Containing an *N*,*O*-Chelating Oxazolylphenolate Ligand

Ho-Jin Son,[a] Won-Sik Han,[a] Kyung-Ryang Wee,[a] Ji-Yun Chun,[a] Kyu-Bum Choi,[a] Su Jung Han,[b] Soon-Nam Kwon,[a] Jaejung Ko,*[a] Chongmok Lee,[b] and Sang Ook Kang*[a]

Keywords: N,O ligands / Boron / Bandgap control / Electrochemistry / Luminescence

A series of four-coordinate boron compounds of the type *N*,*O*-($OPh^{OxZ}ArX$)BPh_2 or *N*,*O*-($OPh^{OxZ}NPh_2$)BPh_2 (**5a**–**g**) has been prepared by treating triphenylboron (TPB) with 2-(4,4-dimethyl-4,5-dihydrooxazol-2-yl)-4-X-arylphenols ($HOPh^{OxZ}ArX$; **4a**–**f**) or 2-(4,4-dimethyl-4,5-dihydrooxazol-2-yl)-4-(4-diphenylamino)phenol ($HOPh^{OxZ}NPh_2$; **4g**). A systematic change in the electronic structures is achieved in these compounds by incorporating electron-withdrawing (EW) and -donating (ED) groups [ArX (X = 4-cyano-, 2,4-difluoro-, 4-chloro-, phenyl, 4-methoxy-, and 4-dimethylaminophenyl) or NPh_2] at the 4-position of the phenoxide. The absorption and emission maxima of the ED groups show a significant red-shift compared to those observed in the EW groups. This red-shift suggests that π-conjugation is effectively extended over the arylphenoxides and oxazoline moiety once the boron center has been plugged into the corresponding ligands. The gradual decrease observed in the bandgaps on going from EW to ED groups is found to be in agreement with the increase in oxidation potentials determined by the cyclic voltammetry (CV) experiments. In particular, a Hammet plot between the EW and ED substituents and oxidation potentials confirms the ground state electronic perturbation. Such alterations are attributed mainly to an elevation of the energy levels of the HOMOs), as further confirmed by a series of theoretical calculations on the frontier orbitals of each system. The ED group (-NPh_2) substituted compound **5g** shows a bipolar character due to intramolecular charge transfer in the complex, with the highest photoluminescence quantum yield being obtained in toluene. This new boron complex was found to function as an emitter in electroluminescence (EL) devices, with a maximum brightness of 2905 cd/m^2 at 13 V and a current efficiency of 1.63 cd/A at 6 mA/cm^2, with a turn-on voltage of 4.3 V.

Introduction

The incorporation of boron atoms into an extended π-aromatic system has attracted considerable attention due to its many applications, such as fluorescent sensors,[1] nonlinear optics,[2] and emitting[3] and electron-transport[4] materials in organic light-emitting devices (OLEDs). Recently, a number of stable three[5]- and four-coordinate[6,7] boron compounds have been reported by several groups and their potential use as electroluminescent materials has been demonstrated. For the production of potential boron-based electroluminescent (EL) materials, it would be beneficial to produce electronically saturated four-coordinate boron compounds where a single ancillary ligand chelates to the boron and functions as a four electron donor with a uninegative charge. The facile formation of four-coordinate boron arises from the initial σ-type interactions between boron and the uninegative heteroatoms of the chelate ligand, followed by dative bonding from the neutral donor atom of the other part of chelate ligand. However, most four-coordinate boron-containing compounds have been limited to three types of chelating ligand system (**A**,[6] **B**,[7] and **C**[8]), as shown in Scheme 1.

This study investigated the *N*,*O*-chelating oxazolylphenoxide ligand system as part of an ongoing search for other uninegative chelating ligand systems. Metal complexes bearing 2-(oxazolyl)phenoxy ligands function as *N*,*O*-chelating ligands and have been used in number of organometallic catalytic systems.[9] However, the use of the oxazoline moiety as a boron-chelating ancillary ligand has not been attempted thus far, particularly in conjunction with the phenoxide system. Recently, we reported that oxazolyl-

[a] Department of Materials Chemistry, Sejong Campus, Korea University,
Chung-Nam 339-700, South Korea
Fax: +82-41-867-5396
E-mail: sangok@korea.ac.kr
[b] Department of Chemistry, Ewha Womans University,
Seoul 120-750, South Korea
Supporting information for this article is available on the WWW under http://www.eurjic.org or from the author.

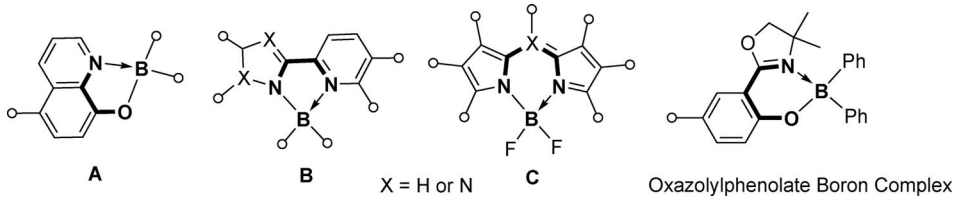

Scheme 1. Four-coordinate boron compounds with an *N*,*O*-/*N*,*N*-chelate ligand.

phenolates are efficient chelating ligands for stabilizing zinc metal, and demonstrated the use of the corresponding zinc complexes as hole-transporting and emitting materials in EL devices.[10] In an effort to use this ligand as an electronically tunable chelate for boron, a series of oxazolylphenols ($OPh^{OxZ}ArX$ and $OPh^{OxZ}NPh_2$; X = 4-cyano-, 2,4-difluoro-, 4-chloro-, phenyl, 4-methoxy-, and 4-dimethylaminophenyl) were synthesized. These modifications allow the photoluminescence properties of the system to be systematically tuned from blue to green (438–520 nm). All chelate compounds **5** show an enhanced PL efficiency when compared to the corresponding chelating ligands **4** as a result of stabilization of the chelating ligand by boron. In particular, the electron-donating moiety (-NPh_2) substituted compound **5g** shows the highest PL efficiency (Φ_f = 34%), thus indicating a bipolar character due to the enhanced charge transfer in the molecule. This paper reports full details of the synthesis and characterization of boron compounds (**5**) of oxazolylphenolates substituted with various electron-withdrawing (EW) and -donating (ED) groups. The corresponding photoluminescence properties have been characterized by UV and PL spectroscopy, and the direct bandgap measured by cyclic voltammetry. Theoretical calculations have been carried out to account for the change in the electronic structures arising from the electron-push and -pull effects on the aryl substituents. Based on the preliminary photoluminescent characteristics of each boron complex, ambipolar **5g** was screened and further tested as an emitting material for multi-layer OLEDs.

Results and Discussion

Synthesis of Boron Compounds 5

Oxazolyl-5-bromophenol (**1**) was prepared from 2-amino alcohol and the carboxylic acid in moderate yield following a literature protocol.[11] Scheme 2 shows the synthesis strategy for the generation of the oxazolylphenol ligands **4a**–**f**. A series of Suzuki-type cross-coupling reactions was performed successfully to yield the benzyl ligands **3a**–**f**, which contain electron-push and -pull functional groups in the 2,4-positions of the aryl units. The desired oxazolylphenol ligands **4a**–**f** were synthesized using a hydrogenolytic deprotection procedure. Finally, a series of electronically tuned four-coordinate boron compounds of the type [*N*,*O*-($OPh^{OxZ}ArX$)]BPh_2 (**5a**–**f**) were synthesized by treating the corresponding oxazolylphenols with triphenylboron (TPB), as shown in Scheme 2. A Pd-catalyzed C–N cross-coupling reaction between the diphenylamine and benzyl ligand (**2**), which was prepared by benzyl protection of **1**, was carried out to yield the diphenylamine-substituted oxazolylbenzyloxybenzene **3g** in good yield. The oxazolylphenol ligand **4g** was prepared by hydrogenolytic deprotection of **3g**. Finally, the desired [2-(4,4-dimethyl-4,5-dihydrooxazol-2-yl)-4-diphenylaminophenolate]diphenylboron (**5g**, **B**–$\mathbf{NPh_2}$) was synthesized by treating one equivalent of **4g** with TPB in thf solution (Scheme 2). All products were isolated by flash chromatography in good yield (81–89%) and were found to be stable to air and moisture both in solution and in the solid state. Single crystals were obtained by recrystallization of the compounds from CH_2Cl_2/hexane (1:2 v/v) solution. Formation of the boron compounds was confirmed by high-resolution mass spectrometry and elemental analyses. All the boron compounds showed the expected signals in the ^1H and ^{13}C NMR spectra, thereby confirming the attachment of the EW and ED functional groups (see Experimental Section).

Structural Characterization of Compounds 5b–5f

X-ray analyses of the five boron compounds **5b** (Figure 1), **5c** (Figure 2), **5d** (Figure 3), **5e** (Figure 4), and **5f**

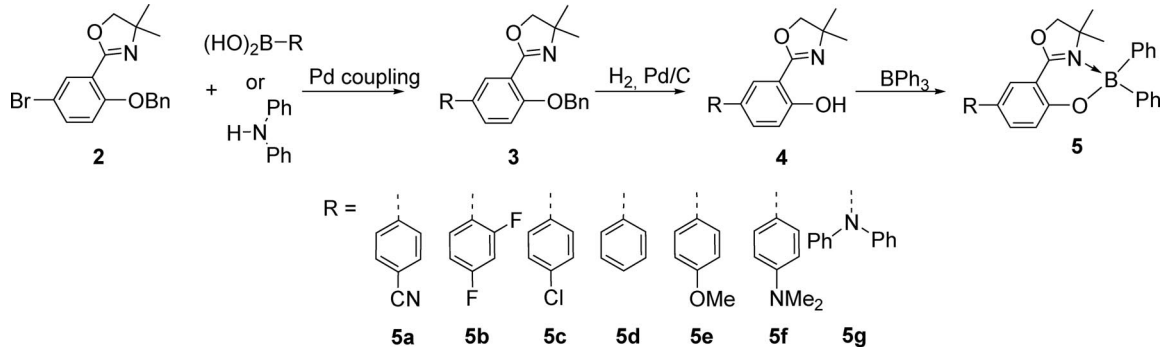

Scheme 2. Preparation of the boron compounds substituted with electron-donating/withdrawing groups (**5a**–**g**).

(Figure 5) were carried out to confirm their structural identity. Each molecule consists of a tetrahedrally coordinated boron atom with two phenyl groups and an *N*,*O*-chelate ligand. The oxazolylphenolate ligands in all five compounds are bound to the boron atom in a similar manner to form a six-membered ring. The B–N, B–O, and B–C bond lengths are similar to those reported elsewhere.[6c,6d,6f] The four bond angles around the boron center reveal a typical tetrahedral geometry (104.2–116.7°), with the boron atom protected by both bulky phenyl groups and the chelating ligand. The N→B–O bite angles of the five compounds are similar to those in previously reported BPh_2q [q = (*N*,*O*)-8-quinolinolate] compounds,[6c,6d,6f] which range from 104.1(1)° to 105.0(1)°. The dihedral angles between the phenolate and aryl rings vary widely according to the 4-substituents. As shown in Table 1, the dihedral angles in compounds bearing ED substituents increase from –9.3(2)° in **5e** to 24.5(3)° in **5f**, whereas the EW substituents give rise to higher dihedral angles ranging from 30.7(7)° in **5d** and 33.8(3)° in **5b** to –40.0(4)° in **5c**. This trend of increasing dihedral angle manifests itself in an interruption of the π-orbital overlap between the two rings. Although none of

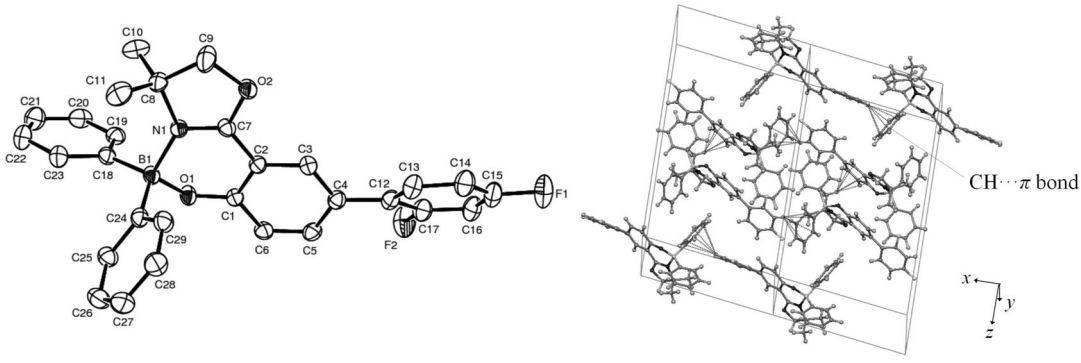

Figure 1. ORTEP drawing (30% probability for thermal ellipsoids) (left) and crystal packing structure (right) of **5b**. The hydrogen atoms have been omitted for clarity.

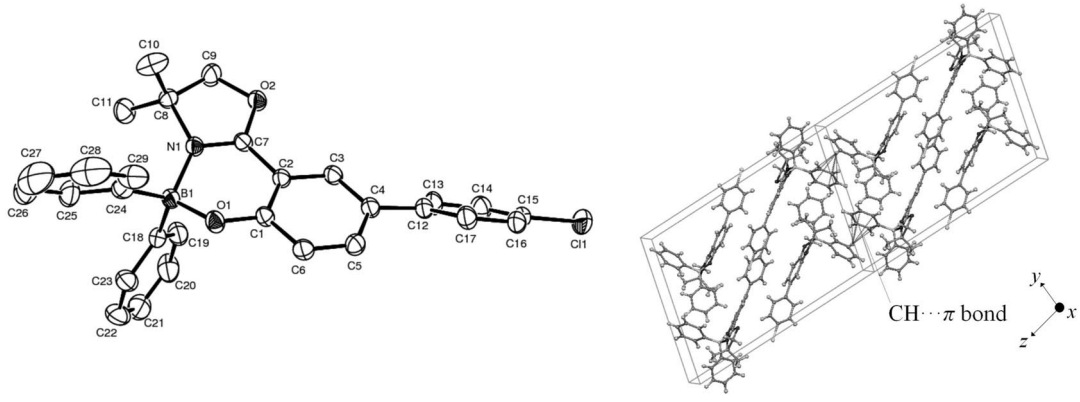

Figure 2. ORTEP drawing (30% probability for thermal ellipsoids) (left) and crystal packing structure (right) of **5c**. The hydrogen atoms have been omitted for clarity.

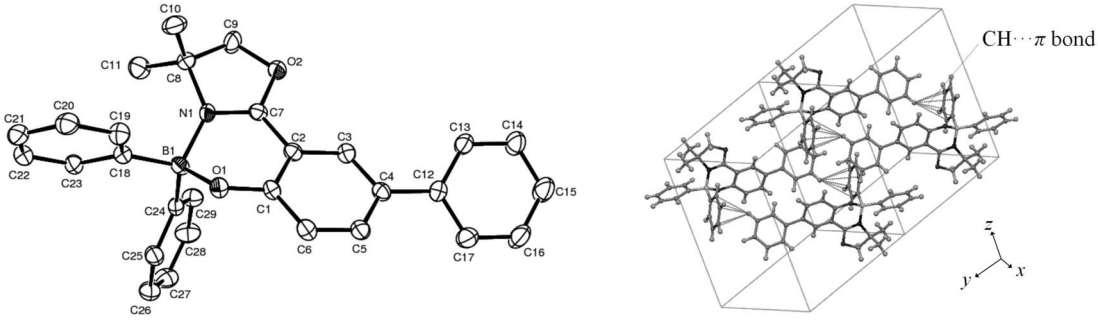

Figure 3. ORTEP drawing (30% probability for thermal ellipsoids) (left) and crystal packing structure (right) of **5d**. The hydrogen atoms have been omitted for clarity.

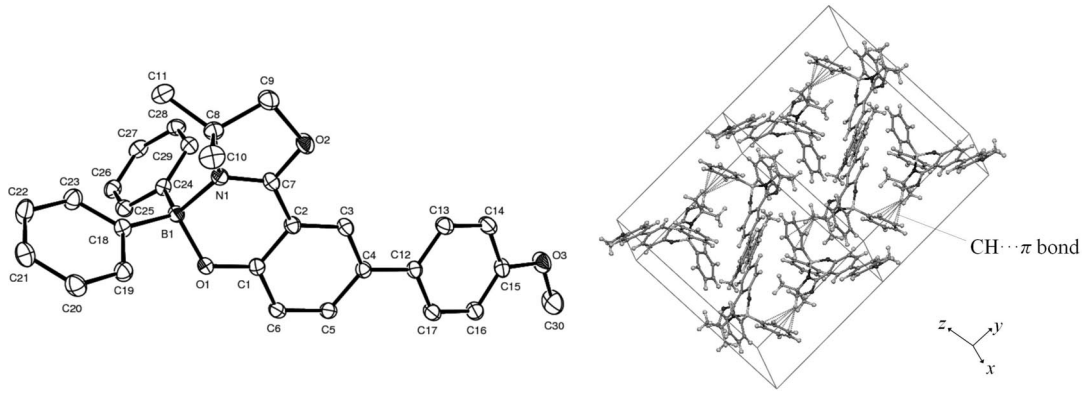

Figure 4. ORTEP drawing (30% probability for thermal ellipsoids) (left) and crystal packing structure (right) of **5e**. The hydrogen atoms have been omitted for clarity.

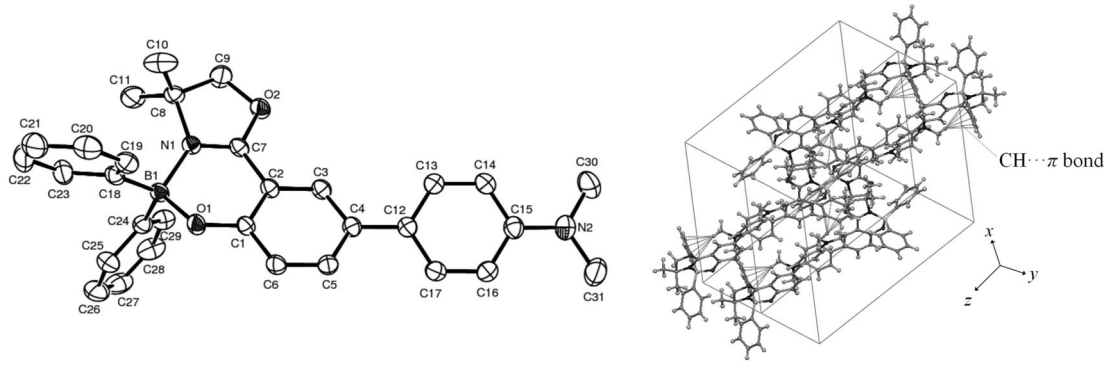

Figure 5. ORTEP drawing (30% probability for thermal ellipsoids) (left) and crystal packing structure (right) of **5f**. The hydrogen atoms have been omitted for clarity.

the compounds show π–π stacking between independent molecules in the crystal due to the absence of co-planarity between the phenyl rings, several CH groups can act as a donors for a CH···π interaction between CH groups and nearby phenyl units. Figures 1–5 clearly show that CH···π interactions are formed efficiently by the CH groups of the alkyl and phenyl substituents as donors and the aromatic ring of aryl substituents as acceptors. Table 2 summarizes these interactions. These values match favorably with those found in other weakly CH···π bonded systems.[12] The distances between the donor H and acceptor π ring, the distances between the donor C and acceptor π ring, and the angles comprising donor H and acceptor C and H of the π ring are in the ranges 2.71–3.00 and 3.56–3.77 Å, and 116.01–125.58°, respectively. This increase in the intermo-

Table 2. Weak CH···π hydrogen bonds in **5b**–**5f**.

Sample	D [Å][a]	D [Å][b]	θ [°][c]
5b	2.762	3.623	123.230
5c	3.00	3.766	121.290
5d	2.954	3.743	116.007
5e	2.710	3.556	125.578
5f	2.706	3.599	120.900

[a] D = H in donor C–H···center of acceptor π ring. [b] D = C in donor C–H···center of acceptor π ring. [c] θ = angle ([H in donor C–H]–[C in acceptor π ring]–[H in acceptor π ring]).

Table 1. Selected bond lengths [Å] and angles [°] in **5b**–**5f**.

	5b	**5c**	**5d**	**5e**	**5f**
B(1)–O(1)	1.519(3)	1.505(3)	1.509(6)	1.509(2)	1.512(2)
B(1)–C(18)	1.613(3)	1.608(4)	1.608(7)	1.616(2)	1.611(3)
B(1)–C(24)	1.618(4)	1.615(4)	1.613(7)	1.627(2)	1.620(3)
B(1)–N(1)	1.620(3)	1.605(3)	1.594(6)	1.607(2)	1.611(2)
C(18)–B(1)–C(24)	117.2(2)	114.7(2)	113.6(4)	114.8(1)	116.7(2)
O(1)–B(1)–C(18)	107.2(2)	108.9(2)	107.4(4)	106.8(1)	105.7(1)
O(1)–B(1)–C(24)	108.0(2)	104.5(2)	109.1(4)	109.6(1)	107.8(1)
O(1)–B(1)–N(1)	104.8(2)	104.4(2)	104.2(3)	104.1(1)	105.0(1)
C(18)–B(1)–N(1)	109.0(2)	110.4(2)	112.2(4)	111.5(1)	110.5(2)
C(24)–B(1)–N(1)	110.0(2)	113.2(2)	109.8(4)	109.5(1)	110.4(1)
C(3)–C(4)–C(12)–C(13)	33.8(3)	–40.0(4)	30.7(7)	–9.3(2)	24.5(3)

lecular interaction induced by cooperative CH···π bonds may be the origin of the increase in thermal stability and high carrier mobility in EL devices.

Thermal Properties

The thermal properties of compounds **5a**–**g** were examined by differential scanning calorimetry (DSC) at temperatures ranging from 30 to 240 °C. Figures 6 and S4 (see the Supporting Information) show the DSC curves for **5g** and **5a**–**f**, respectively. The compounds melted during the first heating phase (180–202 °C), and subsequent heating of the amorphous glassy samples gave rise to glass transition temperatures at 85, 82, and 83 °C for **5g**, **5e**, and **5a**, respectively. Overall, all products showed similar thermal properties due to their similar molecular weights and crystal packing patterns found by X-ray analyses.

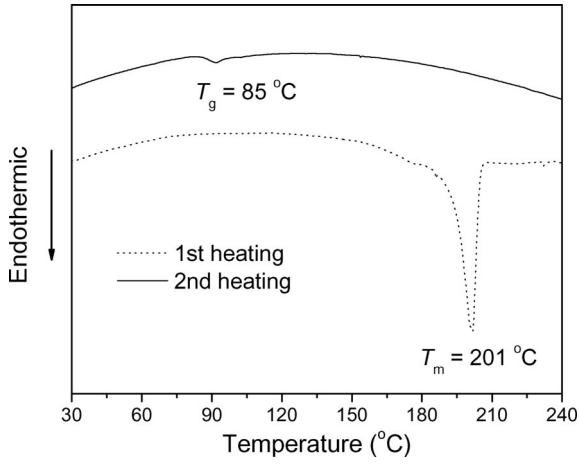

Figure 6. DSC traces of **5g** recorded at a heating rate of 10 °C/min.

Photophysical Properties

The UV/Vis absorption and fluorescence spectra of boron compounds **5** were measured in chloroform. The data are summarized in Table 3. The absorption maxima in the UV/Vis absorption spectra were found to be dependent on the nature of the 4-substituents on the phenolate ligand, and ranged from the UV to visible regions (361–422 nm). Boron compounds **5a**–**g** exhibit a bright luminescence in their fluorescence spectra, with colors ranging from blue to green in solution and in thin film (Figure 7). As shown in Figure 8, the electron-withdrawing substituents (X = CN, F_2, Cl) induce a blue-shift in the emission to 440–453 nm in a thin film, whereas the electron-donating groups (4-dimethylaminophenyl, NPh_2) in **5f** and **5g** cause a red-shift in the emission to 515–527 nm in a thin film. Electron-withdrawing groups apparently increase the energy gap, whereas electron-donating groups decrease the energy gap. The most electron-withdrawing moiety (boron complex **5a**) shows a further blue-shifted PL emission (438 nm in $CHCl_3$).

Table 3. UV/Vis and photoluminescence spectroscopic data for compounds **4** and **5**.

	UV[a] (λ_{max} [nm])	PL (λ_{max} [nm]) solution[a]	film[b]	Stokes shift[a] [cm^{-1}]	Φ_f[c]
4a	299	356, 471	474	12214	0.004
4b	315	363, 469	468	10425	0.003
4c	323	364, 462	461	9316	0.003
4d	322	362, 480	481	10224	0.002
4e	320	365, 495	492	11049	0.001
4f	315	363, 544	531	13365	_[d]
4g	370	420, 553	544	8945	_[d]
5a	361	438	440	4870	0.04(0.05)[e]
5b	362	422	442	3928	0.05(0.03)[e]
5c	368	448	453	4853	0.09(0.10)[e]
5d	369	451	454	4928	0.12(0.10)[e]
5e	374	464	465	5187	0.15(0.12)[e]
5f	385	514(577)[f]	515	6519(8644)[f]	0.10(0.01)[e]
5g	422	520(537)[f]	527	4466(5075)[f]	0.34(0.22)[e] (0.19)[g]

[a] In chloroform. [b] Emission maximum for a thin solid film. [c] In toluene. [d] It was difficult to measure this value due to the low intensity. [e] In CH_3CN. [f] In dmf. [g] Obtained from a comparison of PL intensity in the solid state of the reference compound Alq_3 (22%) and **5g**.

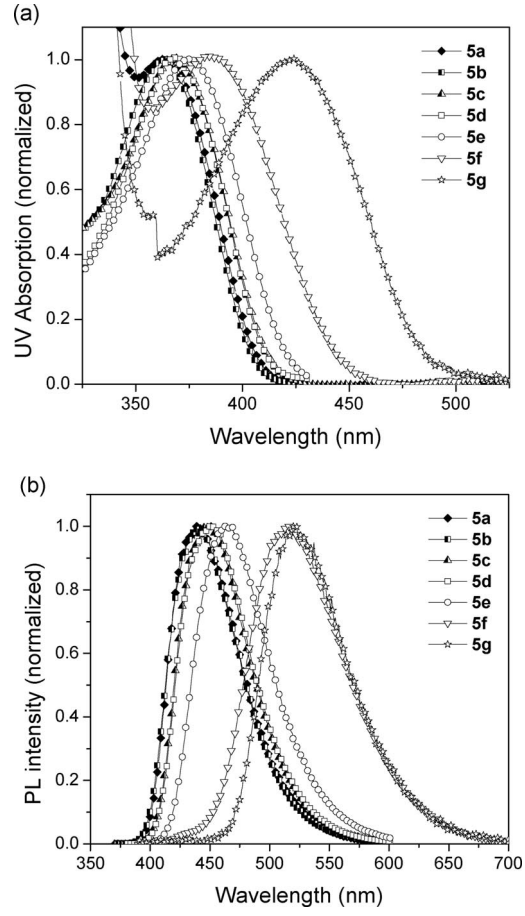

Figure 7. UV/Vis absorption (a) and photoluminescence spectra (b) of compounds **5** in chloroform.

A similar electronic tuning was also observed upon varying the ED and EW substituents at the 4-position of the oxazolylphenol ligands **4**, with panchromatic UV absorption and PL emission maxima in the ranges 299–370 and

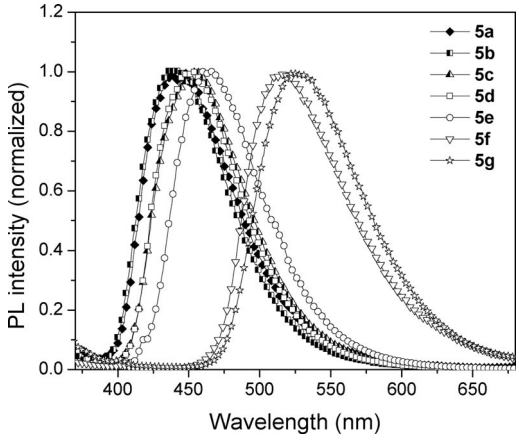

Figure 8. Photoluminescence spectra of compounds **5** in a solid film.

471–553 nm, respectively. In solution, the parent oxazolylphenol ligands **4** undergo an excited state intramolecular proton transfer (ESIPT) process, with characteristic double fluorescence peaks due to facile "enol–keto" tautomerism (see Table 3). In solid films, there appears to be a preference for the keto form, which gives longer wavelength emission. The formation of stable boron chelates **5** effectively blocks this red-shifted low-energy emission pathway found in oxazolylphenol ligands **4**, which exhibit coherent blue-shifted emission spectra.[10] A sharp increase in PL quantum efficiency (Φ_f), with values increasing from 0.001–0.004 to 0.04–0.34, was noted upon boron coordination. This observation is consistent with previous findings on quantum efficiency increase due to restricted ligand flexibility upon metal complexation.[13] As a result of the stabilization by boron coordination, a large positive solvatochromism was observed in the PL emission spectra of the ED-group-substituted compounds **5f** and **5g**, thereby indicating a strong donor-acceptor interaction in the excited state.[14] Both the emission maximum (λ_{max}^{em}) and full width at half-maximum (fwhm) increase dramatically with increasing solvent polarity, for example from λ_{max}^{em} = 482 nm (fwhm = 79 nm) in nonpolar hexane to 577 nm (fwhm = 129 nm) in highly polar dimethylformamide (dmf) in the case of **5f** (Figure 9a). Similar intramolecular charge transfer (ICT) effects were observed in the PL emission of **5g** (Figure 9b). The much larger solvatochromic shifts observed in the PL emission spectra than those observed in the absorption spectra indicate an excited state with a much stronger ICT character and larger dipole moment relative to the ground state in both **5f** and **5g** (Tables S2 and S3 in the Supporting Information). Two different magnitudes of solvatochromic shift (**5f** is 61 nm broader than **5g**) suggest that the dipole moment of the excited state in **5f** is larger than that in **5g**. This is due to the better electronic coupling between the dimethylamine donor and boron acceptor in **5f** than in **5g** and suggests that the donating ability of the dimethylamine moiety in **5f** is superior to that of diphenylamine despite the relatively long conjugation length in phenyl-bridged **5f**.

The fluorescence quantum yields also provide evidence

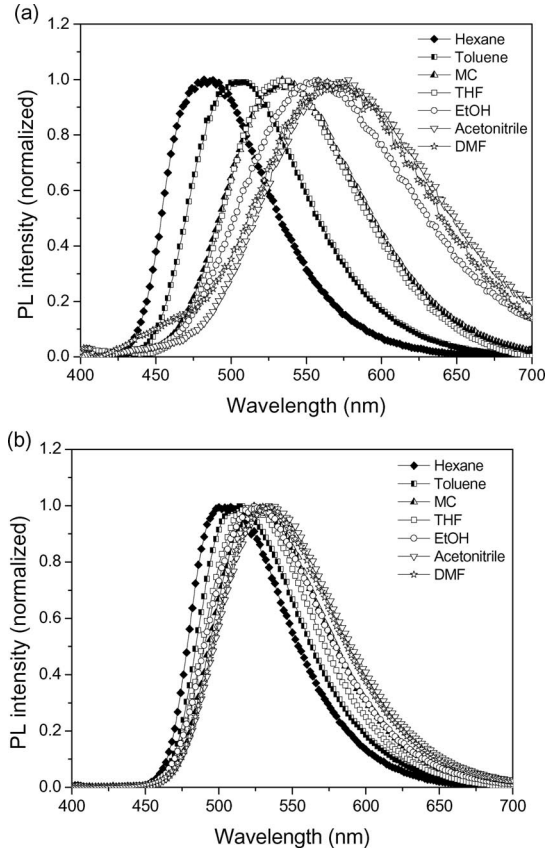

Figure 9. Photoluminescence spectra of **5f** (a) and **5g** (b) in solvents of varying polarity.

for stronger ICT effects in **5f** than in **5g**. Considering that the Φ_f value of a D–A molecule decreases with increasing intramolecular charge transfer,[15] the relatively low Φ_f value of **5f** in toluene shows a larger ICT in its excited state (10% for **5f** vs. 34% for **5g**). As shown in Table 3, more significant ICT emission quenching of **5f** was observed in the highly polar solvent acetonitrile (Φ_f is 10% in toluene and 1% in acetonitrile), thus highlighting its much larger excited-state ICT character. These results confirm that the optical properties of organoboron chelates are significantly dependent on the electronic modification of the chelating ligands.

In general, in accordance with the energy-gap law whereby the non-radiative decay rate constant (k_{nr}) depends exponentially on the energy gap between the singlet and ground states, most metal-chelating compounds[6e,16] show quantum yield decreases with increasing electron density of the ligand, whereas electron-poor moieties cause an increase in both the emission quantum yield and lifetime. In contrast to this prediction, the electron-rich compounds **5e**, **5f**, and **5g** show a relatively high PL quantum yield with respect to their electron-deficient analogues **5a**, **5b**, and **5c**, with values increasing from 4% for **5a** to 34% for **5g** (Table 3). These results can be explained in terms of a developing bipolar character in a rigid planar structure arising from boron coordination, with an intramolecular charge transfer from the electron-donating unit (-OMe, -NMe_2,

-NPh_2) to the electron-accepting oxazoline moiety similar to that reported in thiophene-bridged bipolar compounds.[3c,17]

Electrochemical Properties of 5a–g

The electrochemical properties of boron compounds **5** were examined by cyclic voltammetry (CV). The CV results (in CH_3CN containing 0.1 M tetrabutylammonium hexafluorophosphate at a scan rate of 0.1 $V s^{-1}$) are summarized in Table 4, and some scans are shown in Figure S6 (see Supporting Information). The potential values of the first redox wave, in both the positive and negative directions, of multiple oxidation waves represent E_{ox} and E_{red}, respectively.

As shown in Figures 10 and S6 (Supporting Information), the reversible reduction potentials of **5** were observed at lower values (ca. –0.18 V) than those of the oxazolylphenol ligands **4**. This suggests that coordination of the Lewis acidic boron center to the free ligands significantly stabilizes the LUMO level. A similar role of the boron center has been observed in other organoboron chelate compounds.[18] The reversibility of the redox waves indicates that these boron chelate compounds are electrochemically more stable than the corresponding ligands upon reduction. In the case of the amino-substituted compounds **5f** and **5g**, the aforementioned bipolar character was observed in both oxidation and reduction potential ranges with two reversible oxidation waves (at around 0.7 V) due to the substituted amino groups (Figure 10).

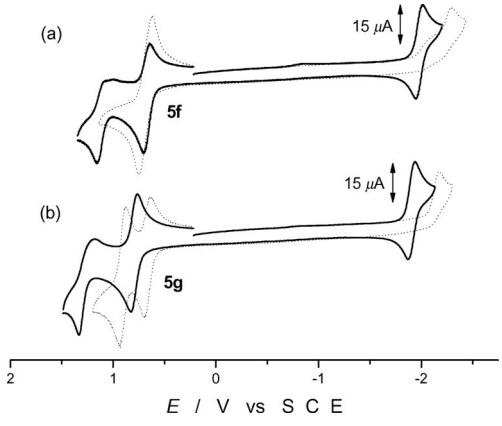

Figure 10. Cyclic voltammograms of 1 mM **5f** [(a), solid line], **4f** [(a), dashed line], **5g** [(b), solid line], and **4g** [(b), dashed line] at a glassy carbon electrode (Φ = 3 mM) in CH_3CN solution containing 0.1 M $TBAPF_6$ at a scan rate of 0.1 $V s^{-1}$.

The HOMO and LUMO energy levels for boron compounds **5** (Figure 11) were calculated from the relationship HOMO/LUMO (eV) = $-e[E_{ox}/E_{red}$ (V vs. SCE) + 4.74 V].[19] The HOMO and LUMO energy levels of **5** were estimated to be –5.42 to –6.30 eV and –2.75 to –2.85 eV, respectively. Overall, the HOMO levels increase on going from electron-withdrawing to electron-donating substituents up to a maximum difference of 0.9 V, whereas the LUMO levels are less sensitive to ligand variations and deviate by only around 0.1 eV.

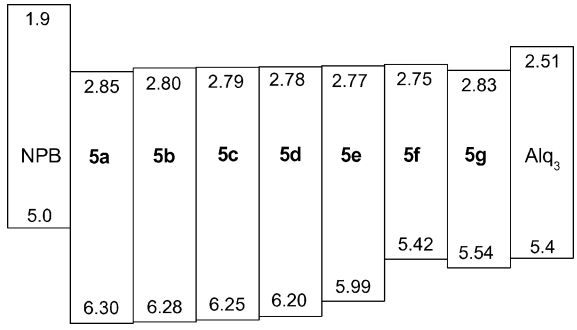

Figure 11. HOMO–LUMO levels of **5** estimated from the cyclic voltammograms.

Similr trends were also found in Hammett plots of the E_{ox} and E_{red} values vs. the σ values of the substituents. As shown in Figure 12, except for **5a**, a good linear relationship (E_{ox} vs. σ) was observed based on the electron-donating/withdrawing substituents on the arylphenolate ring, whereas the plots of E_{red} vs. σ are almost invariant with respect to the ligand substituents. The plots of absorption maximum wavenumber (v_{abs}) and emission maximum wavenumber (v_{em}) vs. ΔE (= $E_{ox} - E_{red}$) show a direct correlation between the HOMO–LUMO bandgaps and the electronic alteration due to the ligand sites, although there is a discrepancy for **5f** (Figure 13). A linear relationship was obtained between v_{abs} and ΔE ($v_{abs} \times 10^4 = 1.764 + 0.303\Delta E$), and the linearity for v_{em} showed a relatively high slope ($v_{em} \times 10^4 = -0.606 + 0.896\Delta E$).

Table 4. Cyclic voltammetry data for compounds **5**.

	Oxidation [V][a]			Reduction [V][a]			[eV]		
	E_{pa1} (E_{pa2})	E_{pc1} (E_{pc2})	$E^{0'}$ [b]	E_{pa1} (E_{pa2})	E_{pc1} (E_{pc2})	$E^{0'}$ [b]	E_g^{el} [c]	HOMO[d]	LUMO[d]
5a	+1.60	–[e]		–1.84	–1.94	–1.89	3.45	–6.30	–2.85
5b	+1.58	–[e]		–1.88	–2.00	–1.94	3.48	–6.28	–2.80
5c	+1.55	–[e]		–1.89	–2.00	–1.95	3.46	–6.25	–2.79
5d	+1.50	–[e]		–1.91	–2.00	–1.96	3.42	–6.20	–2.78
5e	+1.29 (+1.39)	–[e]		–1.95	–1.99	–1.97	3.22	–5.99	–2.77
5f	+0.70 (+1.16)	+0.65 (+1.03)	+0.68 (+1.10)	–1.96	–2.01	–1.99	2.66	–5.42	–2.75
5g	+0.82 (+1.33)	+0.77 (+1.18)	+0.80 (+1.26)	–1.88	–1.94	–1.91	2.71	–5.54	–2.83

[a] E_{pa} = anodic peak potential; E_{pc} = cathodic peak potential. [b] $E^{0'} = (E_{pc} + E_{pa})/2$. [c] E_g^{el} = LUMO – HOMO. [d] HOMO and LUMO levels were determined using the following equations: E_{HOMO} (eV) = $-e(E^{0'} + 4.74)$; E_{LUMO} (eV) = $-e(E^{0'} + 4.74)$. All potentials reported vs. SCE. [e] Not determined due to the lack of reversibility.

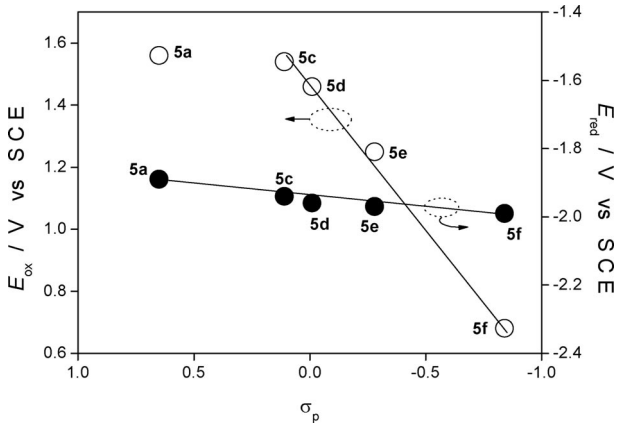

Figure 12. Plots of oxidation (open circle) and reduction (closed circle) peak potentials as a function of the σ_p values of the 4-substituents on the phenyl groups of compounds **5**.

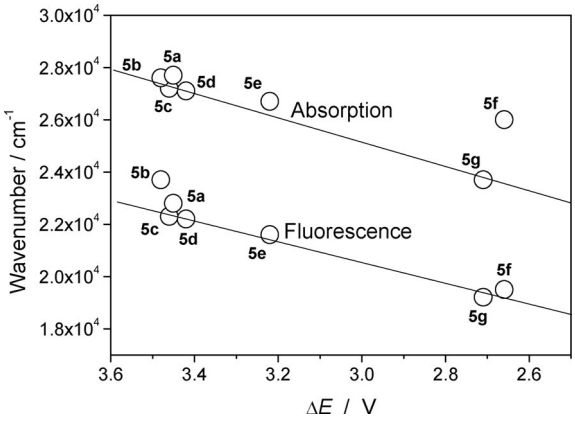

Figure 13. Plots of absorption and emission wavenumbers of compounds **5** as a function of ΔE (= $E_{pa1} - E_{pc1}$).

Theoretical Study of Boron Compounds 5a–g

The electronic structure of these compounds was further investigated by performing quantum chemical calculations at the DFT level of theory, as implemented in the *Dmol*^{3} package.[20] The HOMO–LUMO levels of **5** were calculated using double numerical plus d-functions (DND), and the geometries were optimized under the same conditions. No atom was omitted from the detailed study of the bond lengths and angles of the optimized structure. Figure 14 summarizes the calculated results and representative HOMO and LUMO diagrams for **5d**. The HOMOs of all compounds are mainly located on the arylphenoxide, whereas the LUMOs are found on the oxazolyl and phenolic rings (Figure S7 in the Supporting Information). The frontier orbitals do not show a significant contribution from the boron center, thus suggesting that the HOMO and LUMO energies are dominated by the oxazolylphenolate ligand. In particular, the HOMO energy levels were found to be more susceptible toward aryl substitution than the LUMO energy levels, thereby confirming the variation of each level with values of ΔE = 1.0 eV for the HOMO and ΔE = 0.5 eV for LUMO on going from **5a** to **5g**. This shows that the bathochromic shift observed in the UV and PL spectra is due to an increase in the HOMO levels rather than a decrease in the LUMO levels.

Fabrication of OLED Devices Derived from 5g

The above results suggested that **5g** should be a good emitting material owing to its bipolar character, which benefits the stable injection of holes from the anode and electrons from the cathode. A three-layered device was therefore fabricated with the structure ITO/NPB/**5g**/Alq_3/LiF/Al. As expected, **5g** has potential use as a good emitting material as it displays a maximum brightness of 2905 cd/m^2 at 13 V and a current efficiency of 1.63 cd/A at 6 mA/cm^2 with a turn-on voltage of 4.3 V (Figure 15). However, due to its low PL quantum yield in the solid state (Φ_f = 19%), **5g** has a relatively poor EL performance when compared to other green fluorescent materials.[5c,17,21]

Conclusions

A series of new *N*,*O*-chelate boron compounds where the photophysical properties of each system are modulated by the electron-push and -pull substituents at the 4-position of the oxazolyl phenolates have been prepared. The PL properties and quantum efficiency can be tuned systematically by adding EW and ED groups to the 4-position of the oxazolyl phenolates, with a systematic red-shift and increasing

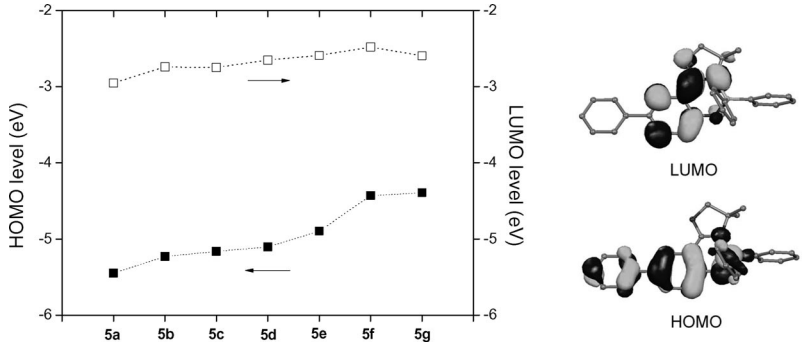

Figure 14. HOMO–LUMO energy levels of **5** and the representative orbital diagram obtained from the *Dmol*^{3} calculation.

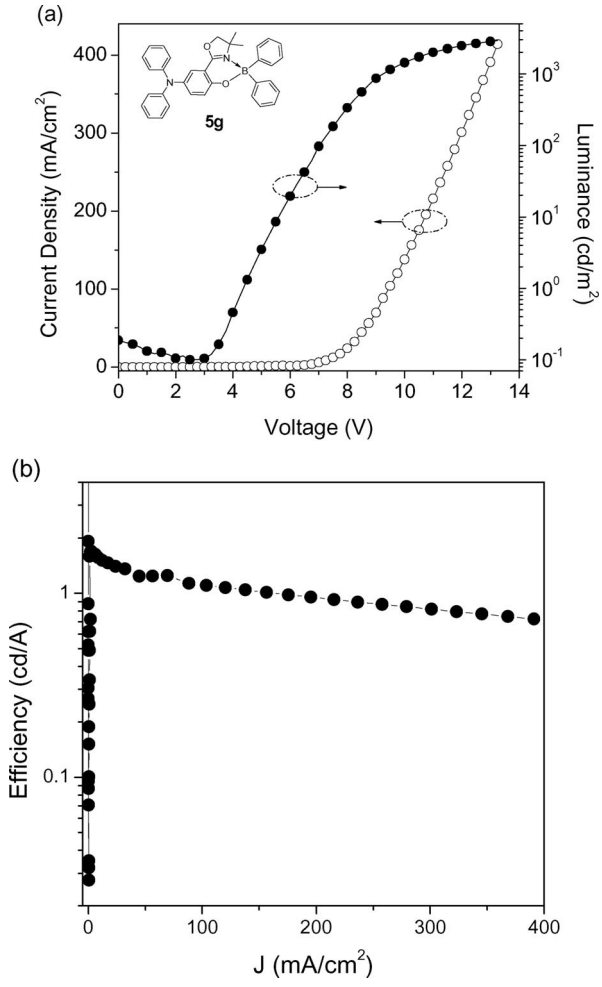

Figure 15. Current density–luminance–voltage characteristics (a) and current efficiency–current density curve (b) of ITO/NPB(50 nm)/**5g**(40 nm)/Alq_3(10 nm)/LiF(0.5 nm)/Al(120 nm).

PL quantum efficiency being obtained upon going from EW to ED groups,. Among this series, **5g** shows the most ambipolar character, with stable electrochemical properties in the CV and a resulting high PL quantum efficiency of 34%. Theoretical calculations have shown that the origin of these enhanced photophysical characteristics is changes in the HOMO level, and that remote electronic control from an arylphenolate ligand system is effective. Subsequent device fabrication with **5g** has revealed a new avenue in the search for good emitting materials for use in OLEDs by electronic tuning of the ligand.

Experimental Section

General Procedures: All manipulations were carried out under a dry nitrogen or argon atmosphere using standard Schlenk techniques. Thf was freshly distilled from potassium benzophenone. The ^1H and ^{13}C spectra were recorded with a Varian unity Inova AS600 spectrometer operating at 599.80 and 150.83 MHz, respectively. All proton and carbon chemical shifts were measured relative to the internal residual benzene from the lock solvent (99.9% $CDCl_3$) and then referenced to Me_4Si (δ = 0.00 ppm). The elemental analyses were carried out using a Carlo Erba Instruments CHNS-O EA 1108 analyzer. High Resolution Tandem Mass Spectrometry (Jeol LTD JMS-HX 110/110A) was performed by the Seoul Branch of the Korean Basic Science Institute. The absorption and photoluminescence spectra were recorded with a SHIMADZU UV-3101PC UV/Vis/NIR scanning spectrophotometer and a VARIAN Cary Eclipse fluorescence spectrophotometer, respectively. The fluorescence quantum yields in toluene and acetonitrile using 9,10-diphenylanthracene as a standard were determined using the dilution method. The cyclic voltammetry (CV) experiments were carried out in CH_3CN containing 1 mM electro-active compounds and 0.1 M tetrabutylammonium hexafluorophosphate ($TBAPF_6$) at room temperature using a BAS 100B electrochemical analyzer. A glassy carbon disk (Φ = 3 mM), platinum wire, and $Ag|AgNO_3$ (0.1 M) were used as the working, counter, and reference electrodes, respectively. All potential values were calibrated vs. the ferrocene/ferrocenium ($Fc|Fc^+$) redox couple, and then corrected to the saturated calomel electrode (SCE) based on an $Fc|Fc^+$ redox potential of 0.38 V vs. the SCE. The thermal stability of boron compounds **5** was measured by DSC (Perkin–Elmer®/Pyris Diamond DSC). A heating rate of 10 °C/min was used after first melting the compound, which was followed by rapid cooling to room temperature. BPh_3, 2-amino-2-methyl-1-propanol, 2-aminoethanol, and 5-bromosalicylic acid were purchased from Aldrich Chemicals and used without purification. $[Pd_2(dba)_3]$ and palladium(II) acetate were purchased from Strem Chemicals. 4,4-Dimethyl-2-[5-(4-Ar)-2-hydroxyphenyl]oxazoline ligands **4a**–**f** were prepared according to the literature method.[10]

Synthesis of 5a: Triphenylboron (0.24 g, 1 mmol) was added to a solution of 2-(4,4-dimethyl-4,5-dihydrooxazol-2-yl)-4-cyanophenylphenol (**4a**; 0.29 g, 1 mmol) in thf (10 mL). After stirring at room temperature for 12 h under N_2, the solvents were evaporated under reduced pressure. The residue was purified by silica gel column chromatography using ethyl acetate/hexane (1:1) as eluent to give **5a** as a white powder. Yield 87% (0.39 g). ^1H NMR ($CDCl_3$): δ = 7.79 (d, $^4J_{H,H}$ = 2.0 Hz, 1 H, *Ph*), 7.65 (d, $^3J_{H,H}$ = 8.4 Hz, 2 H, *Ph*), 7.59 (dd, $^3J_{H,H}$ = 8.8, $^4J_{H,H}$ = 2.4 Hz, 1 H, *Ph*), 7.55 (d, $^3J_{H,H}$ = 8.4 Hz, 2 H, *Ph*), 7.52 (dd, $^3J_{H,H}$ = 7.6, $^4J_{H,H}$ = 1.6 Hz, 4 H, *Ph*), 7.29–7.20 (m, 6 H, *Ph*), 6.99 (d, $^3J_{H,H}$ = 8.8 Hz, 1 H, *Ph*), 4.50 (s, 2 H, CH_2), 1.14 (s, 6 H, CH_3) ppm. ^{13}C NMR ($CDCl_3$): δ = 165.97, 164.03, 147.23, 144.36, 136.08, 134.20, 132.81, 129.02, 127.12, 126.97, 126.81, 125.70, 121.20, 119.14, 110.53, 109.49, 82.34 (CH_2), 66.86, 26.54 (CH_3) ppm. HRMS (FAB) calcd. for $C_{30}H_{25}BN_2O_2$: 456.2009; found 457.2089 $[M + H]^+$. $C_{30}H_{25}BN_2O_2$ (456.34): calcd. C 78.96, H 5.52; found C 78.91, H 5.53.

Synthesis of 5b: A procedure analogous to the preparation of **5a** was used starting from **4b** (0.30 g, 1 mmol). Compound **5b** was obtained as a white powder. Yield 82% (0.38 g). ^1H NMR ($CDCl_3$): δ = 7.70 (s, 1 H, *Ph*), 7.52 (d, $^3J_{H,H}$ = 8.0 Hz, 4 H, *Ph*), 7.48 (dt, $^3J_{H,H}$ = 8.8, $^4J_{H,H}$ = 2.0 Hz, 1 H, *Ph*), 7.30–7.20 (m, 7 H, *Ph*), 6.96 (d, $^3J_{H,H}$ = 8.4 Hz, 1 H, *Ph*), 6.90–6.83 (m, 2 H, *Ph*), 4.42 (s, 2 H, CH_2), 1.10 (s, 6 H, CH_3) ppm. ^{13}C NMR ($CDCl_3$): δ = 166.13, 163.32, 160.97, 158.55, 138.03, 134.29, 131.05, 127.35, 127.12, 126.75, 124.88, 124.29, 120.58, 111.94, 109.10, 104.61, 82.25 (CH_2), 66.72, 26.53 (CH_3) ppm. HRMS (FAB) calcd. for $C_{29}H_{24}BF_2NO_2$: 467.1868; found 468.1955 $[M + H]^+$. $C_{29}H_{24}BF_2NO_2$ (467.31): calcd. C 74.53, H 5.18; found C 74.47, H 5.16.

Synthesis of 5c: A procedure analogous to the preparation of **5a** was used starting from **4c** (0.30 g, 1 mmol). Compound **5c** was obtained as a white powder. Yield 85% (0.39 g). ^1H NMR ($CDCl_3$): δ = 7.70 (d, $^4J_{H,H}$ = 2.4 Hz, 1 H, *Ph*), 7.52 (dt, $^3J_{H,H}$ = 6.4, $^4J_{H,H}$ = 1.6 Hz, 4 H, *Ph*), 7.49 (d, $^4J_{H,H}$ = 2.8 Hz, 1 H, *Ph*), 7.35–7.30

(m, 4 H, *Ph*), 7.29–7.21 (m, 6 H, *Ph*), 6.94 (d, $^3J_{H,H}$ = 8.8 Hz, 1 H, *Ph*), 4.40 (s, 2 H, CH_2), 1.09 (s, 6 H, CH_3) ppm. ^{13}C NMR ($CDCl_3$): δ = 166.20, 163.31, 138.48, 136.17, 134.30, 133.08, 130.08, 129.14, 127.84, 127.16, 126.79, 125.16, 120.89, 109.35, 82.28 (*C*H_2), 66.73, 26.58 (*C*H_3) ppm. HRMS (FAB) calcd. for $C_{29}H_{25}BClNO_2$: 465.1667; found 466.1762 [M + H]$^+$. $C_{29}H_{25}BClNO_2$ (465.78): calcd. C 74.78, H 5.41; found C 74.71, H 5.38.

Synthesis of 5d: A procedure analogous to the preparation of **5a** was used starting from **4d** (0.26 g, 1 mmol). Compound **5d** was obtained as a white powder. Yield 89% (0.38 g). ^{1}H NMR ($CDCl_3$): δ = 7.76 (d, $^4J_{H,H}$ = 2.4 Hz, 1 H, *Ph*), 7.56 (dd, $^3J_{H,H}$ = 8.8, $^4J_{H,H}$ = 2.8 Hz, 1 H, *Ph*), 7.53 (dd, $^3J_{H,H}$ = 8.0, $^4J_{H,H}$ = 2.0 Hz, 4 H, *Ph*), 7.429 (d, $^3J_{H,H}$ = 6.8 Hz, 2 H, *Ph*), 7.335 (t, $^3J_{H,H}$ = 8.0 Hz, 2 H, *Ph*), 7.28–7.18 (m, 7 H, *Ph*), 6.94 (d, $^3J_{H,H}$ = 8.8 Hz, 1 H, *Ph*), 4.32 (s, 2 H, CH_2), 1.05 (s, 6 H, CH_3) ppm. ^{13}C NMR ($CDCl_3$): δ = 166.36, 163.16, 140.05, 136.50, 134.40, 131.46, 129.13, 127.22, 126.83, 126.68, 125.34, 120.80, 109.37, 82.28 (*C*H_2), 66.71, 26.63 (*C*H_3) ppm. HRMS (FAB) calcd. for $C_{29}H_{26}BNO_2$: 431.2057; found 432.2154 [M + H]$^+$. $C_{29}H_{26}BNO_2$ (431.33): calcd. C 80.75, H 6.08; found C 80.69, H 6.07.

Synthesis of 5e: A procedure analogous to the preparation of **5a** was used starting from **4e** (0.30 g, 1 mmol). Compound **5e** was obtained as a yellow powder. Yield 83% (0.38 g). ^{1}H NMR ($CDCl_3$): δ = 7.71 (d, $^4J_{H,H}$ = 2.4 Hz, 1 H, *Ph*), 7.54–7.51 (m, 5 H, *Ph*), 7.36 (dt, $^3J_{H,H}$ = 8.8, $^4J_{H,H}$ = 2.4 Hz, 2 H, *Ph*), 7.27–7.15 (m, 6 H, *Ph*), 6.93 (d, $^3J_{H,H}$ = 8.8 Hz, 1 H, *Ph*), 6.89 (dt, $^3J_{H,H}$ = 8.8, $^4J_{H,H}$ = 2.4 Hz, 2 H, *Ph*), 4.36 (s, 2 H, CH_2), 3.75 (s, 3 H, OCH_3), 1.07 (s, 6 H, CH_3) ppm. ^{13}C NMR ($CDCl_3$): δ = 166.37, 162.69, 159.04, 136.21, 134.35, 132.66, 131.18, 127.69, 127.15, 126.75, 124.70, 120.66, 114.51, 109.27, 82.24 (*C*H_2), 66.62, 55.70 (–O*C*H_3), 26.59 (*C*H_3) ppm. HRMS (FAB) calcd. for $C_{30}H_{28}BNO_3$: 461.2162; found 462.2229 [M + H]$^+$. $C_{30}H_{28}BNO_3$ (461.36): calcd. C 78.10, H 6.12; found C 78.04, H 6.09.

Synthesis of 5f: A procedure analogous to the preparation of **5a** was used starting from **4f** (0.31 g, 1 mmol). Compound **5f** was obtained as a yellow powder. Yield 81% (0.38 g). ^{1}H NMR ($CDCl_3$): δ = 7.71 (d, $^4J_{H,H}$ = 2.4 Hz, 1 H, *Ph*), 7.56 (dd, $^3J_{H,H}$ = 8.4, $^4J_{H,H}$ = 2.4 Hz, 1 H, *Ph*), 7.52 (dd, $^3J_{H,H}$ = 8.0, $^4J_{H,H}$ = 1.6 Hz, 4 H, *Ph*), 7.35 (d, $^3J_{H,H}$ = 8.8 Hz, 2 H, *Ph*), 7.27–7.18 (m, 6 H, *Ph*), 6.92 (d, $^3J_{H,H}$ = 8.8 Hz, 1 H, *Ph*), 6.72 (d, $^3J_{H,H}$ = 9.2 Hz, 2 H, *Ph*), 4.34 (s, 2 H, CH_2), 2.91 (s, 6 H, NCH_3), 1.06 (s, 6 H, CH_3) ppm. ^{13}C NMR ($CDCl_3$): δ = 166.48, 162.28, 149.89, 135.97, 134.39, 131.72, 128.20, 127.28, 127.13, 126.70, 124.08, 120.57, 113.10, 109.26, 82.21, (*C*H_2), 66.56, 40.96 (–N*C*H_3), 26.61 (*C*H_3) ppm. HRMS (FAB) calcd. for $C_{31}H_{31}BN_2O_2$: 474.2479; found 475.2540 [M + H]$^+$. $C_{31}H_{31}BN_2O_2$ (474.40): calcd. C 78.48, H 6.59; found C 78.51, H 6.55.

Synthesis of 4g: A mixture of [Pd_2(dba)$_3$] (0.18 g, 4 mol-%), P(*t*Bu)$_3$ (0.08 g, 8 mol-%), sodium *tert*-butoxide (0.810 g, 15 mmol), 4,4-dimethyl-2-(5-bromo-2-benzyloxyphenyl)oxazoline (**2**; 1.80 g, 5 mmol), and diphenylamine (0.84 g, 5 mmol) was dissolved in toluene (20 mL) and heated to 110 °C for 8 h under nitrogen. After cooling to room temperature, the solution was filtered through a Celite pad. The organic layer was removed under reduced pressure and the residue was purified by silica gel column chromatography using hexane as eluent to give **3g** as a white solid (2.15 g, 96%). The prepared benzyl ligand (**3g**) and a 10% Pd/C catalyst (0.1 g) were dissolved in 30 mL of thf/EtOH (1:1). The mixture was then shaken for 5 h under hydrogen (60 psi) at room temperature. The mixture was filtered through a Celite pad to remove the insoluble catalyst and dried under reduced pressure. The residue was purified by silica gel column chromatography using ethyl acetate/hexane (1:10) as the eluent to give **4g** as a yellow powder. Yield 91% (1.57 g). ^{1}H NMR ($CDCl_3$): δ = 12.12 (s, 1 H, O*H*), 7.44 (m, 1 H, *Ph*), 7.18 (m, 5 H, *Ph*), 7.01 (m, 4 H, *Ph*), 6.93 (m, 3 H, *Ph*), 4.08 (s, 2 H, CH_2), 1.39 (s, 6 H, CH_3) ppm. ^{13}C NMR ($CDCl_3$): δ = 166.00, 156.73, 148.08, 138.85, 132.31, 129.26, 125.73, 125.20, 122.85, 122.03, 118.02, 78.42 (*C*H_2), 28.14 (*C*H_3) ppm. HRMS (FAB) calcd. for $C_{23}H_{22}N_2O_2$: 358.1681; found 358.4337 [M]$^+$. $C_{23}H_{22}N_2O_2$ (358.43): calcd. C 77.07, H 6.19; found C 77.03, H 6.17.

Synthesis of 5g: A procedure analogous to the preparation of **5a** was used starting from **4g** (0.36 g, 1 mmol). Compound **5g** was obtained as a yellow powder. Yield 87% (0.45 g). ^{1}H NMR ($CDCl_3$): δ = 7.46 (d, $^3J_{H,H}$ = 7.2 Hz, 5 H, *Ph*), 7.31–7.27 (m, 5 H, *Ph*), 7.25–7.20 (m, 6 H, *Ph*), 7.02 (d, $^3J_{H,H}$ = 8.4 Hz, 4 H, *Ph*), 6.99–6.94 (m, 3 H, *Ph*), 4.83 (t, 2 H, CH_2), 1.12 (s, 6 H, CH_3) ppm. ^{13}C NMR ($CDCl_3$): δ = 166.06, 160.35, 147.90, 138.30, 136.74, 132.90, 129.45, 127.57, 126.73, 125.30, 123.48, 123.16, 122.42, 121.40, 107.44, 66.51 (*C*H_2), 26.34 (*C*H_3) ppm. HRMS (FAB) calcd. for $C_{35}H_{31}BN_2O_2$: 522.2479; found 523.4197 [M + H]$^+$. $C_{35}H_{31}BN_2O_2$ (522.44): calcd. C 80.46, H 5.98; found C 80.39, H 5.95.

Crystal Structure Determination: Crystals of **5b**–**5f** were obtained from CH_2Cl_2/hexane (1/2, v/v) and mounted on the diffractometer. Preliminary examination and data collection were performed using a Bruker SMART CCD detector system single-crystal X-ray diffractometer equipped with a sealed-tube X-ray source (40 kV, 50 mA) and graphite-monochromated Mo-K_α radiation (λ = 0.71073 Å). The preliminary unit cell constants were determined from a set of 45 narrow-frame (0.3° in ω) scans. The double-pass method of scanning was used to exclude any noise. The collected frames were integrated using an orientation matrix determined from the narrow-frame scans. The SMART software package was used for data collection, and SAINT was used for frame integration.[22a] The final cell constants were determined by a global refinement of the *xyz* centroids of the reflections harvested from the entire data set. The structure solution and refinement were carried out using the SHELXTL-PLUS software package.[22b] Detailed information is listed in Table S1.

CCDC-715202 (for **5b**), -715203 (for **5c**), -715204 (for **5d**), -715205 (for **5e**), and -715206 (for **5f**) contain the supplementary crystallographic data for this paper. These data can be obtained free of charge from The Cambridge Crystallographic Data Center via www.ccdc.cam.ac.uk/data_request/cif.

Fabrication of OLED Devices: OLED devices using compound **5g** as an emitting layer were fabricated. An ITO-coated glass (20 Ω/sq) substrate was first cleaned using conventional procedures. After insertion into a fabrication chamber, the sample was exposed to a UV ozone treatment, and the organic layers were then deposited onto the ITO by thermal evaporation. Finally LiF and Al were deposited successively onto the underlying organic layers. The characteristics of each OLED device were measured using a Photoresearch PR650 spectrometer and a KEITHLEY 306 source measure unit.

Supporting Information (see also the footnote on the first page of this article): The ^{1}H and ^{13}C NMR spectroscopic data for **5**, cyclic voltammograms, UV/Vis, calculation, and PL spectrums for **4** and **5**, and crystal structure data.

Acknowledgments

This study was supported by the Korea Science and Engineering Foundation (KOSEF) through the National Research Laboratory

(NRL) Program funded by the Ministry of Education, Science and Technology (no. R0A-2008-000-200900-2008) and performed in part during a sabbatical year (March 2006–February 2007) at Korea University.

[1] a) M. Kollmannsberger, T. Gareis, S. Heinl, J. Breu, J. Daub, *Angew. Chem. Int. Ed. Engl.* **1997**, *36*, 1333; b) *Chemosensors of Ion and Molecule Recognition* (Eds.: J.-P. Desvergne, A. W. Czarnik), Kluwer: Dordrecht, the Netherlands, **1997**; c) G. Beer, C. Niederalt, S. Grimme, J. Daub, *Angew. Chem. Int. Ed.* **2000**, *39*, 3252; d) S. Yamaguchi, S. Akiyama, K. Tamao, *J. Am. Chem. Soc.* **2001**, *123*, 11372.

[2] a) Z. Yuan, N. J. Taylor, T. B. Marder, I. D. Williams, S. K. Kurtz, L. T. Cheng, *J. Chem. Soc., Chem. Commun.* **1990**, 1489; b) Z. Yuan, N. J. Taylor, T. B. Marder, I. D. Williams, S. K. Kurtz, L. T. Cheng, in *Organic Materials for Non-linear Optics, II* (Eds.: R. A. Hann, D. Bloor), The Royal Society of Chemistry, Cambridge, **1991**, p. 190; c) D. R. Kanis, M. A. Ratner, T. J. Marks, M. C. Zerner, *Chem. Mater.* **1991**, *3*, 19.

[3] a) S. Wang, *Coord. Chem. Rev.* **2001**, *215*, 79; b) Y. Li, Y. Liu, W. Bu, J. Guo, Y. Wang, *Chem. Commun.* **2000**, 1551; c) Y. Shirota, M. Kinoshita, T. Noda, K. Okumoto, T. Ohara, *J. Am. Chem. Soc.* **2000**, *122*, 11021; d) X. T. Tao, H. Suzuki, T. Wada, S. Miyata, H. Sasabe, *J. Am. Chem. Soc.* **1999**, *121*, 9447.

[4] a) T. Noda, H. Ogawa, Y. Shirota, *Adv. Mater.* **1999**, *11*, 283; b) T. Noda, Y. Shirota, *J. Am. Chem. Soc.* **1998**, *120*, 9714.

[5] a) Y. Cui, F. Li, Z.-H. Lu, S. Wang, *Dalton Trans.* **2007**, 2634; b) D. Tanaka, T. Takeda, T. Chiba, S. Watanabe, J. Kido, *Chem. Lett.* **2007**, *36*, 262; c) W. L. Jia, X. D. Feng, D. R. Bai, Z. H. Lu, S. Wang, G. Vamvounis, *Chem. Mater.* **2005**, *17*, 164; d) W. L. Jia, M. J. Moran, Y.-Y. Yuan, Z. H. Lu, S. Wang, *J. Mater. Chem.* **2005**, *15*, 3326; e) Y. Shirota, *J. Mater. Chem.* **2005**, *15*, 75; f) M. Mazzeo, V. Vitale, F. D. Sala, M. Anni, G. Barbarella, L. Favaretto, G. Sotgiu, R. Cingolani, G. Gigli, *Adv. Mater.* **2005**, *17*, 34; g) W. L. Jia, D. R. Bai, T. McCormick, Q. D. Liu, M. Motala, R. Y. Wang, C. Seward, Y. Tao, S. Wang, *Chem. Eur. J.* **2004**, *10*, 994.

[6] a) Y. Nakata, Y. Chujo, *Macromolecules* **2007**, *40*, 6; b) F. Jäkle, *Coord. Chem. Rev.* **2006**, *250*, 1107; c) S. Kappaun, S. Rentenberger, A. Pogantsch, E. Zojer, K. Mereiter, G. Trimmel, R. Saf, K. C. Möller, F. Stelzer, C. Slugovc, *Chem. Mater.* **2006**, *18*, 3539; d) Y. Cui, S. Wang, *J. Org. Chem.* **2006**, *71*, 6485; e) Y. Qin, I. Kiburu, S. Shah, F. Jäkle, *Macromolecules* **2006**, *39*, 9041; f) Y. Cui, Q.-D. Liu, D.-R. Bai, W.-L. Jia, Y. Tao, S. Wang, *Inorg. Chem.* **2005**, *44*, 601; g) X.-Y. Wang, M. Weck, *Macromolecules* **2005**, *38*, 7219; h) Y. Qin, C. Pagba, P. Piotrowiak, F. Jäkle, *J. Am. Chem. Soc.* **2004**, *126*, 7015; i) Q. Wu, M. Esteghamatian, N.-X. Hu, Z. Popovic, G. Enright, Y. Tao, M. D'Iorio, S. Wang, *Chem. Mater.* **2000**, *12*, 79.

[7] a) T.-R. Chen, R.-H. Chien, A. Yeh, J.-D. Chen, *J. Organomet. Chem.* **2006**, *691*, 1998; b) H. Y. Chen, Y. Chi, C. S. Liu, J. K. Yu, Y. M. Cheng, K. S. Chen, P. T. Chou, S. M. Peng, G. H. Lee, A. J. Carty, S. J. Yeh, C. T. Chen, *Adv. Funct. Mater.* **2005**, *15*, 567; c) Q.-D. Liu, M. S. Mudadu, R. Thummel, Y. Tao, S. Wang, *Adv. Funct. Mater.* **2005**, *15*, 143; d) J. J. Klappa, S. A. Geers, S. J. Schmidtke, L. A. MacManus-Spencer, K. McNeill, *Dalton Trans.* **2004**, 883; e) Q. Liu, M. S. Mudadu, H. Schmider, R. Thummel, Y. Tao, S. Wang, *Organometallics* **2002**, *21*, 4743.

[8] a) K. Rurack, M. Kollmannsberger, U. Resch-Genger, J. Daub, *J. Am. Chem. Soc.* **2000**, *122*, 968; b) J. Chen, A. Burghart, A. Derecskei-Kovacs, K. Burgess, *J. Org. Chem.* **2000**, *65*, 2900.

[9] a) A. L. Gott, A. J. Clarke, G. J. Clarkson, I. J. Munslow, A. R. Wade, P. Scott, *Organometallics* **2008**, *27*, 2706; b) S. R. Coles, G. J. Clarkson, A. L. Gott, I. J. Muslow, S. K. Spitzmesser, P. Scott, *Organometallics* **2006**, *25*, 6019; c) I. Westmoreland, I. J. Munslow, A. J. Clarke, G. Clarkson, R. J. Deeth, P. Scott, *J. Organomet. Chem.* **2006**, *691*, 2228; d) R. K. J. Bott, M. Hammond, P. N. Horton, S. J. Lancaster, M. Bochmann, P. Scott, *Dalton Trans.* **2005**, 3611.

[10] H.-J. Son, W.-S. Han, J.-Y. Chun, B.-K. Kang, S.-N. Kwon, J. Ko, S. J. Han, C. Lee, S. J. Kim, S. O. Kang, *Inorg. Chem.* **2008**, *47*, 5666.

[11] H. R. Hoveyda, V. Karunaratne, S. J. Rettig, C. Orvig, *Inorg. Chem.* **1992**, *31*, 5408.

[12] a) I. L. Karle, R. J. Butcher, M. A. Wolak, D. A. da Silva Filho, M. Uchida, J.-L. Bredas, Z. H. Kafafi, *J. Phys. Chem. C* **2007**, *111*, 9543; b) M. Nishio, *Cryst. Eng. Commun.* **2004**, *6*, 130; c) A. Gulyani, R. Srinivasa Gopalan, G. U. Kulkarni, S. Bhattacharya, *J. Mol. Struct.* **2002**, *616*, 103; d) G. R. Desiraju, T. Steiner, *The Weak Hydrogen Bond in Structural Chemistry and Biology, IUCr Series*; Oxford University Press: New York, **1999**; (see pages 140 and 191).

[13] H. Gorner, S. Khanra, T. Weyhermuller, P. Chaudhuri, *J. Phys. Chem. A* **2006**, *110*, 2587.

[14] M. Kollmannsberger, K. Rurack, U. Resch-Genger, J. Daub, *J. Phys. Chem. A* **1998**, *102*, 10211.

[15] a) Z. R. Grabowski, K. Rotkiewicz, W. Rettig, *Chem. Rev.* **2003**, *103*, 3899; b) S. A. Jenekhe, L. Lu, M. M. Alam, *Macromolecules* **2001**, *34*, 7315; c) K. Bhattacharyya, M. Chowdhury, *Chem. Rev.* **1993**, *93*, 507.

[16] a) B. J. Liddle, R. M. Silva, T. J. Morin, F. P. Macedo, R. Shukla, S. V. Lindeman, J. R. Gardinier, *J. Org. Chem.* **2007**, *72*, 5637; b) Y. Qin, I. Kiburu, S. Shah, F. Jäkle, *Org. Lett.* **2006**, *8*, 5227; c) V. A. Montes, R. Pohl, J. Shinar, P. Anzenbacher Jr., *Chem. Eur. J.* **2006**, *12*, 4523; d) R. Pohl, P. Anzenbacher Jr., *Org. Lett.* **2003**, *5*, 2769.

[17] H. Doi, M. Kinoshita, K. Okumoto, Y. Shirota, *Chem. Mater.* **2003**, *15*, 1080.

[18] Y. Cui, S. Wang, *J. Org. Chem.* **2006**, *71*, 6485.

[19] A. J. Bard, L. R. Faulkner, in *Electrochemical Methods: Fundamentals and Applications*, 2nd ed., John Wiley & Sons, **2001**, p. 54.

[20] a) B. Delley, *J. Chem. Phys.* **1990**, *92*, 508; b) B. Delley, *J. Chem. Phys.* **2000**, *113*, 7756.

[21] C.-T. Chen, Y. Wei, J.-S. Lin, M. V. R. K. Moturu, W.-S. Chao, Y.-T. Tao, C.-H. Chien, *J. Am. Chem. Soc.* **2006**, *128*, 10992.

[22] a) *SMART* and *SAINT*, Bruker Analytical X-ray Division, Madison, WI, **2002**; b) G. M. Sheldrick, *SHELXTL-PLUS* Software Package, Bruker Analytical X-ray Division, Madison, WI, **2002**.

Received: January 8, 2009
Published Online: March 12, 2009

